

A Comparison of Multi-Blade Coordinate Transformation and Direct Periodic Techniques for Wind Turbine Control Design

Karl A. Stol¹

The University of Auckland, Auckland, New Zealand

Hans-Georg Moll²

HTWG Konstanz - University of Applied Science, Konstanz, Germany

Gunjit Bir³

National Renewable Energy Laboratory, Golden, Colorado, 80401

Hazim Namik⁴

The University of Auckland, Auckland, New Zealand

The inherent periodic behavior of an operating wind turbine is not well accommodated by common time-invariant analysis and control techniques. A multi-blade coordinate transformation (MBC) helps to overcome this issue for rotors with three or more blades by mapping the dynamic state variables into a non-rotating reference frame. A number of researchers have applied MBC for modal analyses and individual blade pitch controller designs. They do so by assuming the transformed system model from MBC is time-invariant, which is not often the case. The paper explores the validity of the time-invariant assumption by comparison to direct periodic techniques, which retain all periodic system information. In a modal analysis study, eigenvalues of a system after MBC are compared to direct Floquet modes. In an individual blade pitch control design study, a linear quadratic regulation (LQR) design after MBC is compared to direct periodic LQR. A 5-MW three-bladed wind turbine model is used to quantify performance differences. Normal operating conditions are considered as well as conditions selected to increase the harmonics that are unfiltered by MBC. It is found that the direct periodic methods produce almost identical results to time-invariant methods after MBC under all conditions studied. MBC is recommended for three-bladed turbines, which can be followed by Floquet analysis or periodic control design methods if necessary.

Nomenclature

A	=	state matrix
B	=	control input matrix
C	=	output matrix
I_n	=	identity matrix of dimension $n \times n$
J	=	quadratic cost function
K	=	full-state feedback gain
N	=	number of states
N_b	=	number of blades
P	=	number of measured outputs

¹ Senior Lecturer, Department of Mechanical Engineering, Private Bag 92019, AIAA Senior Member.

² Student, Department of Mechanical Engineering, Brauneggerstraße 55.

³ Senior Engineer II, NWTC, Mail Stop 3811, 1617, Cole Blvd., AIAA Senior Member.

⁴ PhD Student, Department of Mechanical Engineering, Private Bag 92019, AIAA Member.

Q, Q'	=	state, output weighting matrices
R	=	input weighting matrix
T_C	=	control input transformation matrix for MBC
T_g	=	generator torque
T_S	=	state transformation matrix for MBC
T_O	=	output transformation matrix for MBC
p	=	per-rotor-revolution
\underline{q}	=	vector of degrees of freedom
\underline{u}	=	control input vector
\underline{x}	=	state vector
\underline{y}	=	measured output vector
Ω	=	rotor speed
ψ	=	blade 1 azimuth angle
θ_i	=	blade i pitch angle

bar above symbol indicates azimuth-averaged
 'NR' subscript relates to the non-rotating frame

I. Introduction

The multi-blade coordinate transformation (MBC) has its origins in the helicopter field^{1,2} for stability analyses. For rotors with three or more blades, this method provides the means to model an inherently periodic system as (an almost) linear time-invariant (LTI) one, thus allowing the use of well-known LTI analysis and control techniques. MBC is also known as the Coleman transformation or Fourier coordinate transformation in literature. For wind turbine modal analysis and control design, the MBC method has only more recently gained interest due to the trend towards use of three-bladed rotors.

The application of MBC for *modal analysis* (via a standard eigenanalysis) of wind turbines has gained the most attention by various authors. Hansen³ and Riziotis⁴ have examined the stability of operating wind turbines, including operation in closed-loop⁵. Bir⁶ demonstrated that incorrect damping information can be obtained from an eigenanalysis without MBC. Bir also reported that MBC alone does not produce a LTI model but rather filters out all periodic terms in the equations of motion except integral multiples of ΩN_b , where Ω is the rotor speed and N_b is the number of blades.

A Floquet modal analysis is required to correctly capture all periodic terms in a wind turbine model, which is the approach used by the authors in the past⁷ (albeit for the structure alone and a two-bladed rotor). Despite the obvious theoretical accuracy, a Floquet analysis has many drawbacks including ambiguity of the modal frequencies and difficulty in identifying modes from modeshapes alone. Conversely, MBC provides far more physical insight to identify modal properties and is possibly the reason it is often favored over the Floquet approach. It is surprising to find that a comparison between the results of a Floquet analysis and MBC eigenanalysis does not appear in wind turbine literature. A brief study of this is included in the paper.

The application of MBC for wind turbine *control design* has had only very recent attention. Van Engelen⁸ formed a time-invariant state-space model using MBC and demonstrated the performance of independent proportional-integral (PI) feedback loops, each designed for different control objectives. Selvam⁹ followed van Engelen's work to describe a multivariable controller, performing the same load reduction tasks with one central control law. Bossanyi¹⁰ uses a reduced form of MBC, a d-q axis transformation, to compare multivariable and independent PI loop control strategies. In all past studies, time-invariant controllers have been applied to an MBC-transformed system. The attraction of MBC in control is in the development of individual blade pitch (IBP) controllers. Via MBC, collective and differential blade pitch signals can be decoupled, which allows different control objectives to be targeted by each signal.

An alternative approach to generate IBP action is to design periodic feedback gains directly from a periodic state-space model, i.e. without a coordinate transformation. This time-varying control technique has been shown in our past studies^{11,12} on two-bladed rotors to give good fatigue damage reduction in the tower, drive-train and blades.

What has yet to be assessed is whether three-bladed rotors would benefit from a direct periodic control method or whether an MBC-based control design is adequate. This comparison is a main feature of the paper.

The next section introduces the nonlinear wind turbine model used for simulation and the construction of linearized models. Section III briefly describes the MBC process, the linear periodic model that results, and discusses the filtering effect of MBC. Sections IV and V compare MBC-based and direct periodic approaches for modal analysis and control design respectively.

II. Wind Turbine Model

To define a typical large wind turbine, we use properties from the NREL 5-MW baseline model¹³, summarized in Table 1. This is a fictitious three-bladed offshore machine that has been used in a number of NREL and international studies. In this paper, the turbine's hydrodynamic properties are not relevant, as if located onshore.

Table 1. Summary of wind turbine properties

Power rating	5 MW
Rotor	3-bladed, upwind
Control	Variable speed, variable pitch
Rotor diameter	126 m
Hub height	90 m
Rated, cut-out wind speed	11.4 m/s, 25 m/s
Rated rotor speed	12.1 rpm

The aeroelastic simulation code FAST¹⁴ (with AeroDyn) is used to linearize the wind turbine model and calculate closed-loop time responses (via MATLAB/Simulink). A variety of degrees of freedom (DOFs) are available in the code to account for flexibility in the tower, drive-train, and blades. Unsteady aerodynamic effects such as dynamic inflow and dynamic stall are possible for time marching simulations but are ignored for linearization.

Steady wind conditions are used for linearization based on the specific operating scenario to be analyzed. These conditions will be described in later sections. Typically, a trim analysis is needed to find the steady collective pitch angles that achieve desired mean rotor speeds. The operating point that is linearized about is periodic in time, with period equal to the time of one rotor revolution.

The result of linearization in FAST of the operating 5-MW turbine is a periodic state-space model, defined by

$$\begin{aligned}\dot{\underline{x}} &= A(\psi)\underline{x} + B(\psi)\underline{u} \\ \underline{y} &= C(\psi)\underline{x}\end{aligned}\tag{1}$$

where $\underline{x} = \begin{bmatrix} q \\ \dot{q} \end{bmatrix}$ is the $N \times 1$ state vector, comprising structural DOFs q (e.g. blade and tower deflections) and their derivatives \dot{q} ,

$\underline{u} = \begin{bmatrix} \theta_1 \\ \theta_2 \\ \theta_3 \end{bmatrix}$ is the vector of individual blade pitch angles (which are assumed the only control inputs),

\underline{y} is the $P \times 1$ vector of turbine measurements,

$A(\psi)$ is the $N \times N$ state matrix, periodic in rotor azimuth angle ψ ,

$B(\psi)$ is the $N \times 3$ control input matrix, and

$C(\psi)$ is the $P \times N$ output matrix.

The complete state-space model includes disturbance terms and possible feed-forward terms but these are not needed for the present study. It should also be noted that \underline{x} , \underline{u} , and \underline{y} describe perturbations from linearization point values, rather than absolute values.

The matrices $\{ A(\psi), B(\psi), C(\psi) \}$ contain the coefficients of the linearized equations of motion, Eqs. (1). Mass, stiffness, and damping properties are contained in $A(\psi)$. The degree that the coefficients are periodic depends on a number of factors, including for example:

- gravity loading, causing variations in blade stiffness during rotation, and
- asymmetric wind inflow (e.g. vertical shear, yaw error), causing variations in blade stiffness and damping.

If one assumes that the periodic variation in the model coefficients is small about mean values, which is rarely the case, then a time-invariant state-space model could be used, such as

$$\begin{aligned}\dot{\underline{x}} &= \bar{A}\underline{x} + \bar{B}\underline{u} \\ \underline{y} &= \bar{C}\underline{x}\end{aligned}\quad (2)$$

where $\{ \bar{A}, \bar{B}, \bar{C} \}$ are calculated by averaging $\{ A(\psi), B(\psi), C(\psi) \}$ over ψ . In such a case, common time-invariant analysis and control design techniques can be applied directly to Eqs. (2). More likely, the periodic variations cannot be ignored, which necessitates MBC (described next) or direct periodic techniques.

III. Multi-Blade Coordinate Transformation of the State-Space Model

MBC transforms coordinates (DOFs, as well as inputs and outputs) that are in the rotating frame of reference into a non-rotating frame. For our three-bladed rotor with example DOF q_i (where i is the blade number), the transformation is defined by:

$$q_i = q_0 + q_c \cos(\psi + \frac{2\pi}{3}(i-1)) + q_s \sin(\psi + \frac{2\pi}{3}(i-1)), \quad i = 1,2,3 \quad (3)$$

where the new coordinates may be called q_0 collective, q_c cosine-cyclic, and q_s sine-cyclic. Note that MBC is a linear transformation because the azimuth angle ψ is prescribed by our linearization point and is not a DOF or state variable.

Using Eq. (3), the state, control input, and output vectors of our linear state-space model, Eqs. (1), can be transformed by

$$\underline{x} = T_s(\psi)\underline{x}_{NR} \quad (4)$$

$$\begin{aligned}\underline{u} &= T_c(\psi)\underline{u}_{NR} \\ \Leftrightarrow \begin{bmatrix} \theta_1 \\ \theta_2 \\ \theta_3 \end{bmatrix} &= \begin{bmatrix} 1 & \cos(\psi) & \sin(\psi) \\ 1 & \cos(\psi + \frac{2\pi}{3}) & \sin(\psi + \frac{2\pi}{3}) \\ 1 & \cos(\psi + \frac{4\pi}{3}) & \sin(\psi + \frac{4\pi}{3}) \end{bmatrix} \begin{bmatrix} \theta_o \\ \theta_c \\ \theta_s \end{bmatrix}\end{aligned}\quad (5)$$

$$\underline{y} = T_o(\psi)\underline{y}_{NR} \quad (6)$$

where \underline{x}_{NR} , \underline{u}_{NR} , and \underline{y}_{NR} now represent states, inputs, and outputs in the non-rotating frame and $\{ T_s(\psi), T_c(\psi), T_o(\psi) \}$ are nonsingular periodic transformation matrices. The elements of $T_s(\psi)$ and $T_o(\psi)$ are omitted for brevity but can be found in Ref 6.

The result is a transformed state-space model:

$$\begin{aligned}\dot{\underline{x}}_{NR} &= A_{NR}(\psi)\underline{x}_{NR} + B_{NR}(\psi)\underline{u}_{NR} \\ \underline{y}_{NR} &= C_{NR}(\psi)\underline{x}_{NR}\end{aligned}\quad (7)$$

The new state matrices $\{ A_{NR}(\psi), B_{NR}(\psi), C_{NR}(\psi) \}$ are typically weakly periodic and one may average them over ψ . This operation gives a linear time-invariant approximation:

$$\begin{aligned}\dot{\underline{x}}_{NR} &= \overline{A}_{NR} \underline{x}_{NR} + \overline{B}_{NR} \underline{u}_{NR} \\ \underline{y}_{NR} &= \overline{C}_{NR} \underline{x}_{NR}\end{aligned}\quad (8)$$

In the MBC process of transforming linear equations of motion from the mixed (rotating plus non-rotating) frame to the purely non-rotating frame, one can observe a filtering effect. Periodic coefficients in the mixed frame may contain, in general, *all* harmonics of the rotor speed. After MBC, only integral multiples of 3p (for a 3-bladed rotor) exist. The intermediate harmonics (1p, 2p, 4p, etc.) do not disappear during MBC, they contribute to the remaining harmonics: 0p (mean), 3p, 6p, etc. An example that has been studied both analytically and numerically to support this observation is the case of a turbine operating in a vacuum with only gravity loading. Gravity gives rise to a 1p variation in the $A(\psi)$ matrix from blade stiffness terms. After MBC, $A_{NR}(\psi)$, contains only 3p periodic variations (plus 0p). The same is true for any 1p and 2p variations in $A(\psi)$ regardless of the physical source, e.g. wind shear. A summary of how harmonics are redistributed when applying MBC is provided in Table 2, which has been generated by systematic application of MBC in MATLAB.

Table 2. Redistribution of harmonics due to MBC filtering

		Harmonics in the non-rotating frame			
		0p	3p	6p	...
Harmonics in the mixed frame	0p	•			
	1p	•	•		
	2p	•	•		
	3p	•	•		
	4p	•	•	•	
	5p	•	•	•	
	6p	•		•	
...					

IV. Modal Analysis Comparison

The objective of the modal analysis comparison is to investigate the extent of modal data inaccuracy using MBC and averaging compared to a direct periodic approach. We compare the following three approaches for calculating modal data.

1. Eigenanalysis before MBC:
Eigenvalues of \overline{A} in Eqs. (2), i.e. averaging performed before MBC.
2. Eigenanalysis after MBC:
Eigenvalues of \overline{A}_{NR} in Eqs. (8), i.e. averaging performed after MBC.
3. Direct Floquet Modal Analysis:
Characteristic exponents of $A(\psi)$ in Eqs. (1) using Floquet theory.

The first approach is the most straightforward in that no application of MBC or Floquet theory is necessary. This approach has been illustrated by Bir⁶ to give erroneous stability results for a wind turbine operating in extreme yawed conditions. The simple approach is included in the present study to observe any issues for normal operating conditions. The second approach is that taken by many researchers³⁻⁶, whether the averaging is intentional or as a consequence of the model used. The third approach is theoretically most sound but is more computationally intensive and problematic. The problems arise when calculating the damped natural frequencies because they are

indeterminate by a multiple of the rotor frequency. A study of time responses can help to overcome this problem. Details of Floquet theory for the modal analysis of wind turbines can be found in Ref. 7. Using either of the three approaches, the modal data is a set of N complex modes, from which the damped natural frequency and damping ratio can be extracted for each complex conjugate mode pair.

Two wind turbine operating conditions are examined. The first is a normal operating case, chosen because it represents an operating point typically chosen by control designers. The second operating condition is chosen from the International Electrotechnical Commission (IEC) design standard¹⁵ specifically to maximize the periodic coefficients in the MBC-transformed system, thereby reflecting a worst case scenario for averaging. A summary of the wind and turbine configuration for each case is summarized in Table 3.

Table 3. Operating cases for modal analysis comparison

	Normal Operating Case	Extreme Operating Case
Basis	Typical control design point	IEC load case 6.2a, idling
Hub-height wind speed	18 m/s	50 m/s
Vertical shear exponent	0.2	0.2
Yaw error	0°	60°
Rotor speed	12.1 rpm (rated)	0.1 rpm
Collective blade pitch	15°	90°
Generator torque/power	rated	0

A. Normal Operating Case

The normal operating case is based on a typical control design point: full power generation with a hub-height wind speed of 18 m/s midway between rated and cut-out speeds. The model uses 15 active DOFs, which are all those allowable in FAST except yaw. The DOFs include: tower fore-aft and side-side bending (1st and 2nd assumed modes), rotor azimuth, shaft torsion, blade flap bending (1st and 2nd modes), and blade edge bending (1st mode).

All underdamped modes are presented in Table 4, ordered from low to high frequency. The key result is that there is no significant difference between modal data calculated by Floquet and an eigenanalysis after MBC; the modal frequencies and damping ratios are the same for all modes. The largest relative difference is in the damping ratio of the blade 2nd flap regressive mode (0.5%). It was anticipated that the vertical wind shear present would cause some differences in the modal data but this has not been the case.

Table 4. Modal data for the normal operating case

Mode	Eigenanalysis before MBC		Eigenanalysis after MBC		Floquet Modal Analysis	
	Frequency [Hz]	Damping Ratio [%]	Frequency [Hz]	Damping Ratio [%]	Frequency [Hz]	Damping Ratio [%]
Blade 1 st flap regressive	0.74	61.5	0.29	87.3	0.29	87.2
Tower 1 st side-side	0.33	0.4	0.32	0.6	0.32	0.6
Tower 1 st fore-aft	0.33	6.8	0.33	8.1	0.33	8.1
Blade 1 st flap collective	0.52	70.1	0.52	70.2	0.52	70.2
Blade 1 st flap progressive	0.74	61.9	0.70	60.7	0.69	60.9
Blade 1 st lag regressive	1.13	4.4	0.88	1.3	0.88	1.3
Blade 1 st lag progressive	1.15	4.0	1.29	0.9	1.29	0.9
Drivetrain twist	1.68	2.5	1.68	2.5	1.68	2.5
Blade 2 nd flap regressive	2.31	14.1	1.72	21.7	1.72	21.6
Blade 2 nd flap collective	2.00	17.8	2.00	17.8	2.00	17.8
Blade 2 nd flap progressive	2.32	14.1	2.12	17.4	2.12	17.4
Tower 2 nd fore-aft	2.77	0.9	2.89	1.9	2.89	1.9
Tower 2 nd side-side	2.94	1.2	2.94	1.2	2.94	1.2
Blade 1 st lag collective	3.98	6.0	3.98	6.0	3.98	6.0
Yaw	5.79	3.9	6.08	4.5	6.07	4.5

The first approach (eigenanalysis before MBC), also produced reasonable data for most of the modes. Large differences are only found in the blade progressive/regressive modes in which the rotor plane precesses in the non-

rotating reference frame. The asymmetric nature of these modes can explain why they are indistinguishable if $A(\psi)$ is averaged.

B. Extreme Operating Case

In the extreme operating case the turbine is in a parked configuration with blades fully feathered. The yaw error of 60° was chosen to be large enough to provide high asymmetric aerodynamic loads while avoiding a potential violation of the aerodynamic model assumptions in AeroDyn for yawed flow. The rotor speed is fictitious (not calculated from open-loop simulation) but also not unrealistic under the conditions. The motivation behind a slow rotor speed is to maximize the relative effect of gravity loading on the blade stiffness compared to centrifugal stiffening. The resultant 1p variation in stiffness gives rise to 3p variations in $A_{NR}(\psi)$, as described in Section III. Combined with the anticipated high blade damping variations from high speed yawed flow, the extreme operating case has the biggest potential to generate a significantly periodic $A_{NR}(\psi)$. Fewer FAST DOFs (tower fore-aft and side-side bending (1st mode) and blade flap bending (1st mode)) than in the previous case were chosen to simplify the analysis.

All modal data is presented in Table 5. Note that due to the high yaw error in this case, there is significant coupling between the blade flap states in the modeshapes. Therefore, traditional mode labels of ‘flap collective’, ‘flap progressive’, and ‘flap regressive’ could not be applied. The labels ‘flap mode 1’, ‘flap mode 2’, and ‘flap mode 3’ were used instead, which were identified between modal analysis methods by state contributions in the modeshape vectors.

The maximum difference between modal data calculated by Floquet and an eigenanalysis after MBC was a 21% relative difference in damping ratio of one of the blade flap modes. While this difference is certainly larger than in the previous normal operating case, on an absolute scale it clearly does not lead to different stability conclusions.

Other operating cases were considered (such as low wind speed, different yaw error, and larger vertical shear) but none produced a significant difference between an eigenanalysis after MBC and Floquet results. Therefore, the use of Floquet for a three-bladed turbine does not appear warranted. To be conservative, an analyst would be best to perform MBC, then examine the periodic variations in $A_{NR}(\psi)$. If variations are small (presently subjective), then a Floquet analysis could be deemed unnecessary. If periodic variations are large, then a Floquet analysis should follow MBC to take advantage of the improved system conditioning⁶.

Table 5. Modal data for the extreme operating case

Mode	Eigenanalysis before MBC		Eigenanalysis after MBC		Floquet Modal Analysis	
	Frequency [Hz]	Damping Ratio [%]	Frequency [Hz]	Damping Ratio [%]	Frequency [Hz]	Damping Ratio [%]
Tower 1 st fore-aft	0.32	2.3	0.31	3.1	0.31	3.1
Tower 1 st side-side	0.33	0.33	0.33	0.33	0.33	0.32
Blade 1 st flap mode 1	0.67	14.2	0.65	12.9	0.65	15.1
Blade 1 st flap mode 2	0.67	14.2	0.67	16.7	0.67	13.8
Blade 1 st flap mode 3	0.68	13.5	0.70	12.0	0.70	12.7

V. Control Design Comparison

In this section, the design of a LTI controller after MBC is compared to a periodic controller designed by a direct method. The goal is to determine whether a direct periodic controller that accounts for all periodic effects offers any performance advantages over the LTI controller, which is a simpler design. The control application chosen for the comparison is individual blade pitch for fatigue load reduction as this is a common scenario in literature using MBC.

The normal operating case in Table 3 of Section IV defines the linearization point about which a linear state space model is constructed. Five FAST DOFs are chosen: tower fore-aft bending (1st mode), rotor azimuth, and blade flap bending (1st mode). Closed-loop time simulations are conducted with a constant hub-height wind speed of 18 m/s and a step change of vertical shear exponent from 0.0 to 0.2 after 30 seconds. This simple wind input is effective enough for controller comparisons without requiring full-field turbulent wind inputs. The influence of nonlinearities while operating away from the linearization point is beyond the scope of the study.

The architecture of the closed-loop system is shown in Fig. 1. The *Power Controller* block contains two conventional control elements, typical in variable-speed wind turbine designs. The first element is a fixed gain proportional-integral (PI) controller, which generates collective pitch angles $\underline{\theta}^o$ to regulate the rotor/generator speed Ω to the rated value. The second element is a constant generator torque command. More complex power controllers featuring, for example, gain scheduling is not required when simulating with a constant wind speed. Structural load control is not an objective of the power controller; this function is performed by the IBP controller. Simulations are run with the power controller operating alone, which is referred from this point as the Baseline controller for normalizing results.

The *IBP Load Controller* block in Fig. 1 represents either of the multivariable controllers under investigation. The individual pitch angles \underline{u} are added to the collective pitch angles from the power controller to result in total instantaneous pitch commands $\underline{\theta}$.

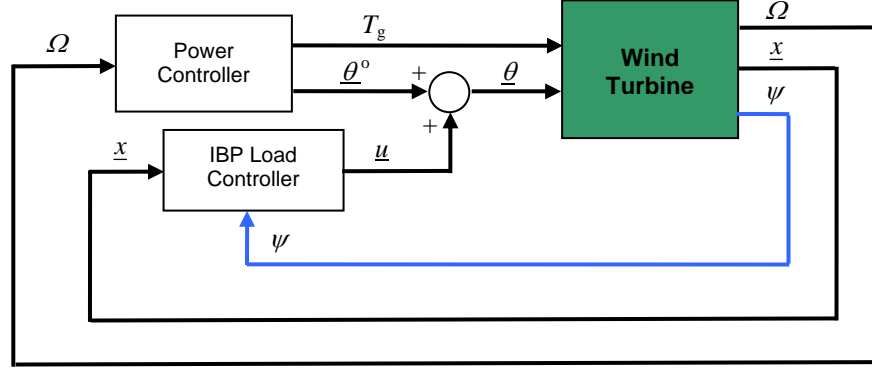


Figure 1. Block diagram of the closed-loop system

The design process for the two main IBP controllers are described next. Simulation results are then presented for two separate control objectives: (1) mitigation of shaft bending fatigue, and (2) mitigation of tower fore-aft bending fatigue. The two objectives serve to illustrate different features of the two control design approaches.

A. Time-Invariant Control Design after MBC

Given the LTI state-space model after MBC and averaging, Eqn. (8), there are many linear control design methods available. Linear quadratic regulation (LQR) is the method chosen in this study because it incorporates all dynamic coupling between transformed states. LQR is an optimal design method which minimizes a quadratic cost function as a trade-off between state regulation and control input (i.e. blade pitch) usage:

$$J = \int_0^{\infty} \left(\underline{x}_{NR}^T Q_{NR} \underline{x}_{NR} + \underline{u}_{NR}^T R_{NR} \underline{u}_{NR} \right) dt \quad (9)$$

where Q_{NR} is the $N \times N$ weighting on states and R_{NR} is the 3×3 weighting on control inputs. In the present study it is more convenient to trade-off output regulation, giving rise to the new cost function:

$$J = \int_0^{\infty} \left(\underline{y}_{NR}^T Q'_{NR} \underline{y}_{NR} + \underline{u}_{NR}^T R_{NR} \underline{u}_{NR} \right) dt \quad (10)$$

where Q'_{NR} is the $P \times P$ output weighting matrix. Eqns. (9) and (10) are equivalent when $Q_{NR} = C_{NR}^T Q'_{NR} C_{NR}$.

With numerical LQR tools, we calculate the state full-state feedback gain K_{NR} in

$$\underline{u}_{NR} = -K_{NR} \underline{x}_{NR} \cdot \quad (11)$$

From Eqns. (4), (5) and (11), the control law in terms of the original rotating coordinates can be formed:

$$\begin{aligned}\underline{u} &= -T_C(\psi)K_{NR}T_S(\psi)^{-1}\underline{x} \\ &= -K_{MBC}(\psi)\underline{x}\end{aligned}\tag{12}$$

where $K_{MBC}(\psi) = T_C(\psi)K_{NR}T_S(\psi)^{-1}$, a $3 \times N$ periodic gain matrix. Thus, MBC produces a periodic control law although this fact is often disguised if the transformation and inverse transformation are performed during run-time.

B. Direct Periodic Control Design

Unlike with LTI systems, there are relatively few control design methods available for periodic systems. Periodic linear quadratic regulation (PLQR) does exist and has been successfully applied to wind turbines in the past^{11,16}. Following a similar approach for LTI systems, with PLQR we may define an output weighting matrix $Q(\psi) = C(\psi)^T Q' C(\psi)$ and input weighting matrix R to calculate the full-state feedback gain $K_{PLQR}(\psi)$ in Eqn. (13), although now we use the periodic state-space model Eqn. (1) directly.

$$\underline{u} = -K_{PLQR}(\psi)\underline{x}\tag{13}$$

As with the MBC-based control design approach, we assume that the wind turbine states \underline{x} are available for feedback, as shown in Fig. 1. The design of an observer or Kalman filter to estimate the state vector is not within the scope of the current study.

C. Results for Objective 1: reduce shaft bending fatigue

The first control design case considers the single IBP control objective of reducing fatigue damage due to low-speed shaft (LSS) bending. This is chosen because it is a common objective amongst researchers using MBC for control design of three-bladed turbines. By reducing the cyclic bending loads in the LSS, one also reduces yaw and tilt moments at the nacelle yaw bearing. The objective is interesting from a controls perspective because it requires an influence over asymmetric rotor thrust loads, which is only feasible by pitching the blades individually.

To satisfy the control objective, we select two measured outputs,

$$\underline{y} = \begin{bmatrix} \text{LSS tilt moment} \\ \text{LSS yaw moment} \end{bmatrix}$$

and give each an equal weighting in the LQR and PLQR designs (i.e. $Q'_{NR} = \alpha I_2$, $Q' = \alpha' I_2$, and $R_{NR} = R = I_3$, where α and α' are scalars for tuning). A check of the open- and closed-loop pole map on the complex plane, Fig. 2, reveals that damping has been added to the asymmetric flap modes as desired. Also, feedback is not influencing the rotor speed, tower fore-aft, or collective flap modes, which as intended by the control design. The PLQR controller has virtually the same pole map (not shown).

A plot of selected gains of $K_{MBC}(\psi)$ for blade 1, Fig. 3, shows surprisingly that the gains are weakly periodic. This is due to desiring an equal influence over tilt and yaw moments, which restores polar symmetry. The same result would be achieved if PI loops were used for tilt and yaw moments in the non-rotating frame instead of the full-state feedback approach. Essentially, this implies that a simple time-invariant controller could perform the same task as either of the two periodic designs. This hypothesis will be proven shortly.

Simulations were performed for 60 sec and analyzed between 30 and 60 sec for root-mean-square (RMS) speed error, LSS tilt moment fatigue damage equivalent load (FDEL), LSS yaw moment FDEL, and RMS pitch rate. This short analysis period is sufficient for steady winds. In Table 6 are the performance results for each IBP load controller, normalized to the baseline (power control only) results. The controller labeled *LTI* is a full-state feedback controller with a constant gain matrix calculated by azimuth-averaging $K_{MBC}(\psi)$.

It is clear from the tabled results that the LTI controller performs just as well as both the (weakly) periodic PLQR and MBC-based controllers for mitigating shaft bending fatigue. There is in fact little difference between the performance of all three controllers. The lesson learned from this test case is that not all IBP control problems require periodic gains.

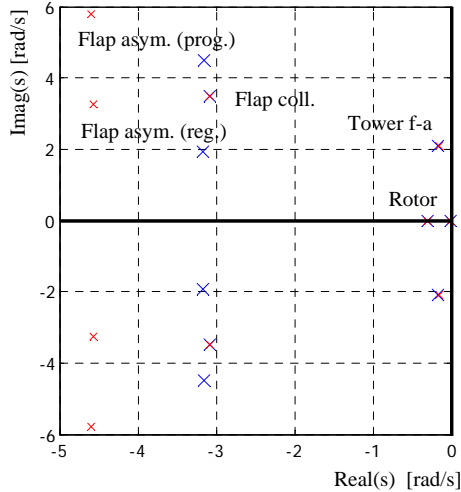


Figure 2. Open- and closed loop pole map for the LQR after MBC controller, Objective 1.
Large blue crosses: open-loop modes. Small red crosses: closed-loop modes.

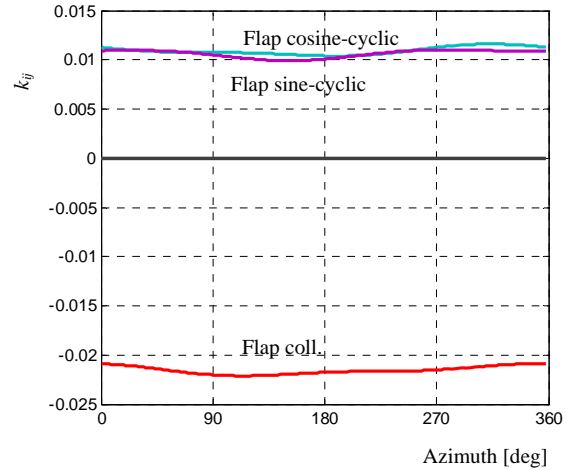


Figure 3. Selected blade 1 pitch gains for the LQR after MBC controller, Objective 1

Table 6. Normalized performance results for Objective 1: reduce shaft bending

Performance Measure	Baseline	Load Controller		
		LTI	LQR after MBC	PLQR
RMS speed error	1.00	1.12	1.12	1.18
LSS tilt moment FDEL	1.00	0.55	0.55	0.55
LSS yaw moment FDEL	1.00	0.40	0.39	0.38
RMS pitch rate	1.00	49.6	49.5	49.3

If either the tilt or yaw moment is weighted more than the other in the control design then polar symmetry would be lost and the generated gains would be (more strongly) periodic. This situation was analyzed to find that still the PLQR and LQR after MBC designs perform virtually identically. The reason for this is that the state matrices after MBC $\{A_{NR}(\psi), B_{NR}(\psi), C_{NR}(\psi)\}$ are weakly periodic and averaging them does not lose any significant model information. This led us to search for other control problems where averaging may not be so advantageous.

D. Results for Objective 2: reduce tower fore-aft bending fatigue

The second control design case is intended to investigate a situation where there is a larger periodic variation in the state matrices after MBC compared to the previous case. The objective now is to reduce cycling bending loads in the tower base in the fore-aft direction. Typical modern controllers would achieve this objective via collective pitch and the symmetric thrust loads that are influenced. With this approach, one would have to consider the impact on speed regulation and ideally design a collective pitch controller for speed and tower motion simultaneously. For purposes of illustration, the present study requires that tower fore-aft loads be regulated by cyclic pitch (asymmetric rotor thrust) only. This should then ensure that speed regulation by the power controller is not influenced by IBP.

This second design case is a good candidate for study because it was found that elements of $B_{NR}(\psi)$ are highly periodic, specifically those that relate to the tower fore-aft equation of motion. A plot of these elements is presented in Fig. 4. One can observe that the periodic variations are dominated by $3p$ but higher multiple harmonics are also present.

For the control design, a single measured output is used: $y =$ Tower base fore-aft bending moment. Then, output and input weightings are selected for the LQR after MBC controller. What is immediately apparent is the need to add weighting for the collective pitch usage (the 1-1 entry in R_{NR}) to ensure a cyclic pitch controller is produced. The pole map in Fig. 5 shows that damping has indeed been introduced to the tower fore-aft bending mode without influencing the rotor speed or collective flap poles. A small amount of coupling with the flap asymmetric modes is

also noticeable. This is expected because we are using IBP to influence asymmetric rotor thrust. Unlike the previous case, the gains in $K_{MBC}(\psi)$ are highly periodic, Fig 6. In fact, they are centered roughly on zero, which implies that averaging to generate an LTI controller is fruitless.

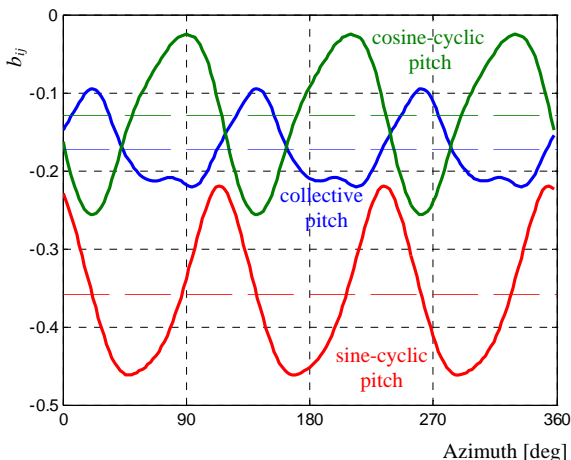


Figure 4. Periodic elements of $B_{NR}(\psi)$ for the tower fore-aft equation, Objective 2. Dashed lines: mean values.

Performance results from simulation are listed in Table 7. The LTI controller presented is identical to the one designed for the previous case (for LSS tilt and yaw moments). It is included to illustrate that an LTI controller must necessarily couple yaw and tilt, and therefore is incapable of reduced tower fore-aft loads without sacrificing pitch usage.

The PLQR controller clearly performed worse compared to the LQR controller after MBC, even after tuning. The reason is that the design is made in the mixed frame and so the collective pitch usage could not be isolated and minimized, unlike with the LQR controller. Consequently the PLQR IBP controller generates collective pitch commands to dampen the tower motion, which interferes with the speed regulation.

In order to include the periodic terms neglected by the LQR controller, PLQR must follow MBC rather than be applied directly. Following this approach led to the last column of results in Table 7. These results are almost identical to those from LQR after MBC, which suggests as in the previous cases that little information is lost by averaging after MBC.

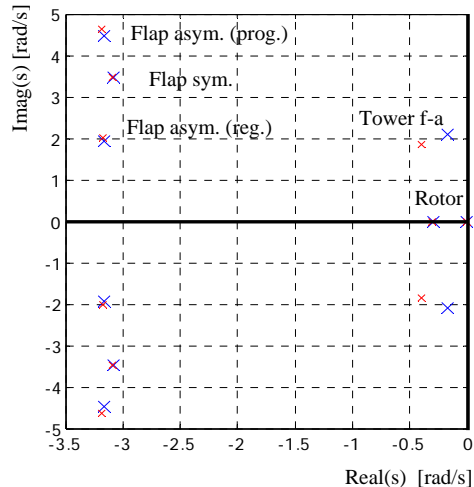


Figure 5. Open- and closed loop pole map for the LQR after MBC controller, Objective 2. Large blue crosses: open-loop modes. Small red crosses: closed-loop modes.

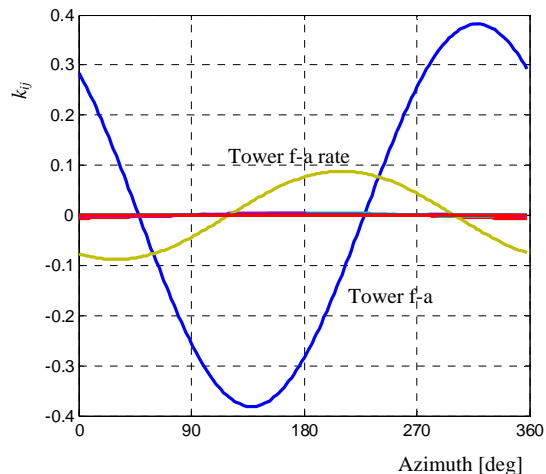


Figure 6. Selected blade 1 pitch gains for the LQR after MBC controller, Objective 2.

Table 7. Normalized performance results for Objective 2: reduce tower fore-aft bending

Performance Measure	Baseline	Load Controller			
		LTI	LQR after MBC	PLQR	PLQR after MBC
RMS speed error	1.00	1.12	1.06	1.13	1.06
Tower fore-aft FDEL	1.00	0.58	0.57	0.63	0.57
LSS tilt moment FDEL	1.00	0.55	0.67	0.79	0.66
LSS yaw moment FDEL	1.00	0.40	1.02	0.97	0.98
RMS pitch rate	1.00	49.6	29.2	30.5	29.1

VI. Conclusions

This paper presented a discussion of the multi-blade coordinate transformation (MBC), which is used primarily to remove periodic coefficients from three-bladed wind turbine models. The source of periodic coefficients in the equations of motion was discussed as well as how these are filtered by MBC to result in periodic coefficients with only 3p, 6p, 9p, etc. harmonics. To assess whether the transformed system can be accurately represented as a time-invariant one by averaging, two specific applications were investigated: modal analysis of operating turbines and individual blade pitch control design. Comparisons were made to direct periodic techniques for analysis and control synthesis using a 5-MW wind turbine model.

In the modal analysis study, an eigenanalysis of the turbine model after MBC was compared to a direct Floquet modal analysis. Both a normal operating case and an extreme operating case were considered. In both cases, modal data compared very closely between the two analysis methods. A maximum relative difference of 21% in damping ratio was reported in the extreme operating case but this was still not considered significant in an absolute sense.

In the control design study, linear quadratic regulators (LQRs) were designed for the turbine model after MBC and compared to direct periodic LQR designs. Two different control objectives were considered separately and performance was quantified in simulation. In both cases, the periodic LQR designs performed no better.

For any three-bladed wind turbine analysis, MBC is a valuable first step in filtering out periodic coefficients. In possibly very rare circumstances, such as with two-bladed rotors, the transformed system will still have significant periodic terms remaining. On these occasions, the periodic methods discussed in this paper (Floquet and periodic LQR) may help to further deal with the system.

VII. References

- ¹Coleman, R. P. and Feingold, A. M., "Theory of self-excited mechanical oscillations of helicopter rotors with hinged blades," *NACA Technical Report TR 1351*, 1958.
- ²Johnson, W., *Helicopter Theory*, Princeton University Press, New Jersey, 1980.
- ³Hansen, M. H., "Improved modal dynamics of wind turbines to avoid stall-induced vibrations," *Wind Energy*, Vol. 6, Issue 2, 2003, pp. 179-195.
- ⁴Riziotis, V. A., Voutsinas, S. G., Politis, E. S., and Chaviaropoulos, P. K., "Aeroelastic stability of wind turbines: The problem, the methods, and the issues," *Wind Energy*, Vol. 7, Issue 4, 2004, pp. 373-392.
- ⁵Riziotis, V. A., Politis, E. S., Voutsinas, S. G., and Chaviaropoulos, P. K., "Stability Analysis of Pitch-regulated, Variable Speed Wind Turbines in Closed Loop Operation Using a Linear Eigenvalue Approach," *Journal of Physics: Conference Series, The Science of Making Torque from Wind*, Lyngby, Denmark, 2007.
- ⁶Bir, G., "Multi-Blade Coordinate Transformation and Its Applications to Wind Turbine Analysis," *Proceedings of the AIAA Wind Energy Symposium*, Reno, Nevada, 7-10 January 2008.
- ⁷Stol, K., Bir, G., & Balas, M., "Floquet Modal Analysis of a Teetered-Rotor Wind Turbine," *ASME J. Solar Energy Engineering*, Vol. 124(4), 2002, pp. 364-371.
- ⁸van Engelen, T. G., "Control design based on aero-hydro-servo-elastic linear models from TURBU (ECN)," *Proceedings of the European Wind Energy Conference*, Milan, 2007.
- ⁹Selvam, K., Kanev, S., van Wingerden J. W., van Engelen, T., and Verhaegen, M., "Feedback-feedforward Individual Pitch Control for Wind Turbine Load Reduction," *Int. J. Robust Nonlinear Control*, Vol. 19, p72-91, 2009.
- ¹⁰Bossanyi, E.A., "Individual Blade Pitch Control for Load Reduction," *Wind Energy*, Vol. 6, pp. 119-128, 2003.
- ¹¹Stol, K. & Balas, M., "Full-State Feedback Control of a Variable-Speed Wind Turbine: A Comparison of Periodic and Constant Gains," *ASME J. Solar Energy Engineering*, vol. 123(4), 2001, pp. 319-326.
- ¹²Stol, K. A., W. Zhao, and Wright, A. D., "Individual Blade Pitch Control for the Controls Advanced Research Turbine (CART)," *ASME J. Solar Energy Engineering*, Vol. 128(4), 2006, pp. 498-505.
- ¹³Jonkman, J., Butterfield, S., Musial W., and Scott, G., "Definition of a 5-MW Reference Wind Turbine for Offshore System Development," NREL/TP-500-38060, National Renewable Energy Laboratory, Golden, CO, 2007.
- ¹⁴Jonkman, J. and M. Buhl Jr, "FAST User's Guide," NREL NREL/EL-500-38230, 2005.
- ¹⁵IEC 61400-1 Ed. 3, *Wind Turbines – Part 1: Design Requirements*, International Electrotechnical Commission (IEC), 2005.
- ¹⁶Liebst, B. S., "A Pitch Control System for the KaMeWa Wind Turbine," *J. Dynamic Systems, Measurement, and Control*, Vol. 107, 1985, pp. 47-52.